Proceedings of the 29th Annual International
Conference of the IEEE EMBS
Cité Internationale, Lyon, France
August 23-26, 2007.

Development of real-time motion artifact reduction algorithm for a wearable photoplethysmography

Hyonyoung Han, Min-Joon Kim, and Jung Kim

***Abstract*— This paper presents a motion artifact reduction algorithm for a real-time, wireless and wearable photoplethysmography (PPG) device for measuring heart beats. A wearable finger band PPG device consists of a 3-axis accelerometer, infrared LED, photo diode, a microprocessor and wireless module. Sources of the motion artifacts were investigated from the hand motions, through computing the correlations between the three directional finger motions and distorted PPG signals. A two-dimensional active noise cancellation algorithm was applied to compensate the distorted signals by motions, using the directional accelerometer data. NLMS (Normalized Least Mean Square) adaptive filter (4th order) was employed in the algorithm. As a result, the signals' distortion rates were reduced from 52.34% to 3.53%, at frequencies between 1 and 2.5 Hz, which representing daily motions such walking and jogging. The wearable health monitoring device equipped with the motion artifact reduction algorithm can be integrated as a terminal in a so-called ubiquitous healthcare system, which provides a continuous health monitoring without interrupting a daily life.**

I. Introduction

PULSATION, as a vital signal, adequately creates a health care monitoring and an emergency health alarm device since it can be easily measured in our bodies. Photoplethysmography (PPG) [1] is a noninvasive pulse signal measurement instrument, which has the potential to be developed into a portable device due to its relatively small sensor size. The PPG sensor detects pulse waves from vessel volume changes using a photoelectric device. Changes in heart beat, blood pressure and vessel cross section affect optical reflection rates. Using these properties, pulsation, which is related to heart beat, can be acquired by gathering reflected light.

Currently, the instrument is used, and was developed for, diagnosis in the hospital or at home. However, the size of the device, the real-time measurement, wireless system and motion artifacts present problems in developing a portable, U-health care system device. In particular, motion artifacts present the most challenging problem; accordingly many methods were researched to overcome this hindrance. There are two main categories; one is software approaches which analyze the pulsation component with frequency and time domain analysis methods [2-4]. But most of them compensate off-line data signals, and their program size is so large that the device can not be worn. Another approach is the hardware approach, which removes the motion artifacts, using body movement information derived from other motion acquisition sensors. New approach is the model-based noise cancelling techniques [5]. They use nonlinear filter for reducing noise, cause of its non-stationary condition. But they need use both another motion tracking sensor and signal processing step for reducing motion artifacts. The most well-known method of the hardware approach is active noise cancellation algorithm with an adaptive filter [6, 7]. However, coefficient orders of the filter are too large to worn the device, and experiments are mostly wired communication.

This paper presents a real-time, wireless and wearable device with a motion artifact reduction algorithm, which has an applicable programming size for portable devices. Active noise cancellation algorithm compensates the corrupted signals by using body movement data from a 3-axis accelerometer.

The organization of this paper is as follows. Section 2 describes the constitution of the device; the hardware description and applied algorithm theory used to reduce motion artifacts is explained. Experiments are described in section 3; confirmation of correlations between noise and motion are experimented with, and a signal reconstruction algorithm is applied to evaluate the compensation rate. Finally, a conclusion is given in section 4.

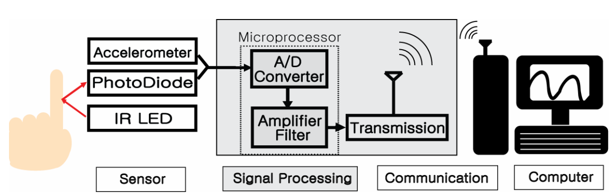

Fig. 1. Block diagram of photoplethysmography

Manuscript received June 22, 2007. This work was supported by the Korea Science and Engineering Foundation(KOSEF) grant funded by the Korea government(MOST) (No. R01-2007-000-11659-0).

Hyonyoung Han is with the Department of Mechanical Engineering, Korea Advanced Institute of Science and Technology, Daejeon, Korea (hhn98@kaist.edu).

Min-Joon Kim is with H3 system, Daejeon, Korea, (e-mail: mjkim@h3system.co.kr).

Jung Kim is an assistant professor at the Department of Mechanical Engineering, Korea Advanced Institute of Science and Technology, Daejeon, Korea (e-mail: jungkim@kaist.edu).

II. Design

A. Hardware description

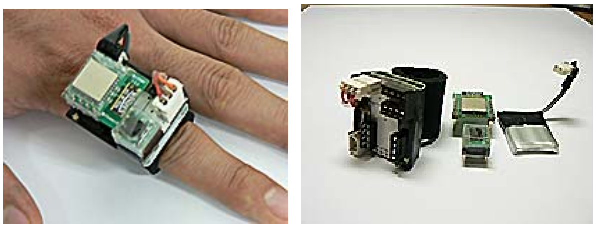

Fig. 2.Wearable PPG sensor

The PPG device is shown in Fig. 1. The sensor part is composed of an infra-red LED, a photo diode for a PPG sensor, and a 3-axis accelerometer for measuring body motion. High order signal processing is necessary due to the noise components, such as light from the surrounding environment, power noise and the DC component in the raw data signal. Signal processing is consisted not only on the circuit but also in the microprocessor to reduce the weight of the device. This improved signal is transmitted to a host computer with a Bluetooth wireless communication.

The device (25 x 30 mm^2, 16.8g) is attached to the finger base as a finger band, as shown in Fig. 2. The optical sensor is located on the inner layer of the band, and the accelerometer is on the circuit. A Bluetooth module is used as a wireless protocol, and a lithium polymer battery is used as a power source. PIC16F876A converts analog signals to digital with 10 bit resolution and contains digital signal processing algorithms. On the signal processing part, the filter is designed as a 0.5 – 3 Hz band pass filter (2nd order analog active filter and 1st order digital Butterworth filter), considering that an average of the human's pulsation is 0.8 – 2 Hz.

B. Motion artifact reduction algorithm

This research compensates the corrupted pulsation signal using body movement data which is strongly related to the motion artifacts. Fig. 3 shows a block diagram of an active noise cancellation algorithm, which reconstructs a raw pulsation signal (sk) from the corrupted signal (dk), using measurable noise signal (xk). Here, PPG and body motion data correspond to dk and xk respectively. This research predominantly used 3-axis accelerometer signals (xk) for body motion data (nk).

In this study, NLMS (Normalized Least Mean Square)

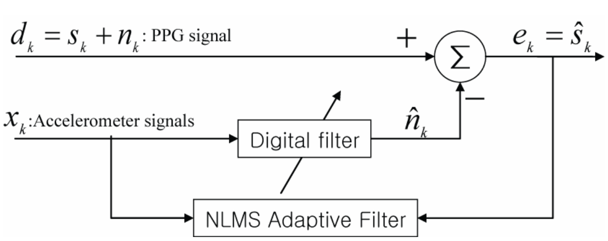

Fig. 3. Active noise cancellation algorithm

adaptive filters were employed due to their fast processing and low order filter coefficients [8]. In the equation (1), w(n), the digital filter coefficient is computed from products of step size (μ(n)), input data (x(n)) and error data (e(n)). Instead of fixed step size in LMS algorithm, the step size are changed and normalized by the energy of input data vector. Step size, μ, are computed with the coefficients a, b and input data as equation (2), and the role of the coefficients are prevent the step size not to fluctuate excessively. Thorough this various step size condition, in NLMS cases, more flexible and stable signal processing is possible, which is appropriate for real-time and wireless sensors.

$$\mathbf{w}(n+1) = \mathbf{w}(n) - \boldsymbol{\mu}(n)\mathbf{x}(n)e(n) \quad (1)$$

$$\boldsymbol{\mu}(n) = \frac{b}{a + \mathbf{x}^{\mathbf{T}}\mathbf{x}} \quad (2)$$

C. Evaluation

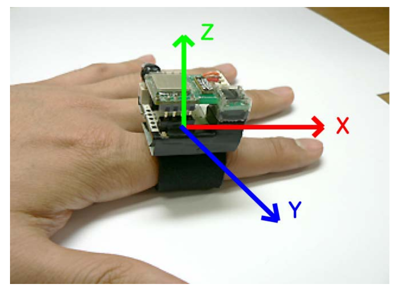

Fig. 4. Coordinate system

Cross-correlation (C.C.) and zero-crossing (Z.C.) counting methods are applied to analyze distortion and compensation rates of the measured PPG signal. The value of the C.C. evaluates a similarity between two different signals. In this case, the signal distortion rate of each axial direction can be obtained by analyzing the C.C. value between the corrupted signal and the reference signal during the motion. Pulse counting methods, Z.C., can detect pulse/min and the amount of pulsation. By using this figure we can analysis the distortion rate.

III. Experimental

A. Classification of the motion artifact

Signal distortions were analyzed on each axial directional motion condition, such as shown in Fig. 4. Experimental conditions were 2 Hz frequency and 20 cm distance motions over 30 seconds. The designed device is worn on the left index finger, and motionless signals are obtained using the right hand as a reference signal.

On the motionless condition, the C.C. between the reference and the measurement signal is 0.9 and the Z.C. difference of those signals is 0. This means that they have a strong relationship. However x, y directional result shows that they have a very weak relationship, due to the fact that its C.C value is less than 0.4, and the Z.C. difference is more

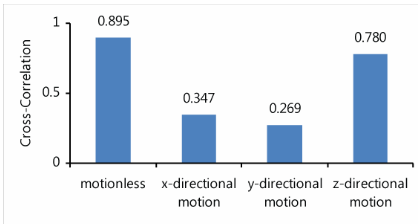

(a)

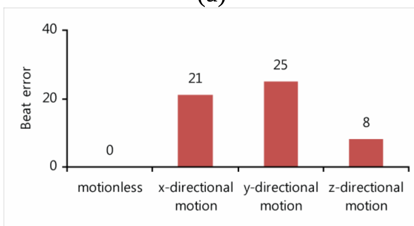

(b)

Fig. 5. (a) Correlation between reference and measured signals (b) Error of zero-crossing during motions during 30s

than 20. The reason for that is, the x-direction goes in the same direction as the blood vessels and the blood flow in the finger. The effect of y-direction can be regarded by the concentration of weight and the momentum of the device. On account of its concentrated weight, the device is easy to rotate during the motion.

Accordingly in this research, x and y directional motions are applied as sources of a compensation algorithm.

B. *Classification of the motion artifact*

To analyze the characteristic of motion and signal distortion, experiments were conducted on x directional motion of the various conditions (frequency: 0 - 2.5 Hz, distance : 0 - 30 cm).

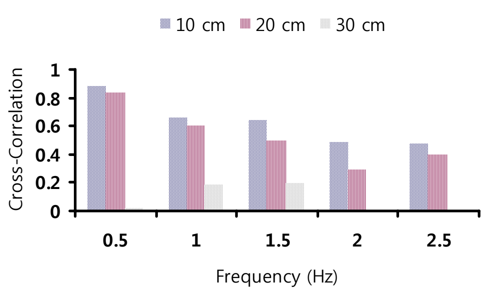

(a)

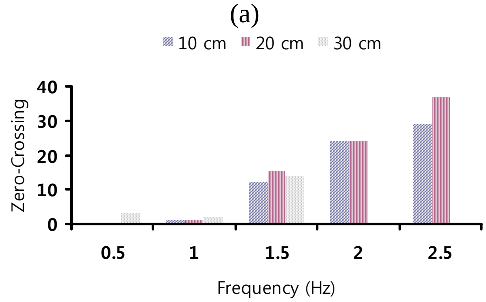

(b)

Fig. 6. (a) Correlation between reference and measured PPG (b) Difference between each zero-crossing value under various conditions

The graph represents C.C. values (Fig. 6(a)) and the difference of Z.C. counts (Fig. 6(b)) between the reference and the measured PPG signal in various conditions. As a result, there is an approximately stable condition under 1 Hz and below a 20 cm distance. Consequently, we can conclude that there is little effect on a condition slower than the pulsation frequency. In contrast, frequencies higher than 1 Hz, and distances longer than 30 cm can create serious signal distortions. Therefore, we apply these seriously corrupted conditions to the motion artifact reduction algorithm.

C. *Motion artifact reduction*

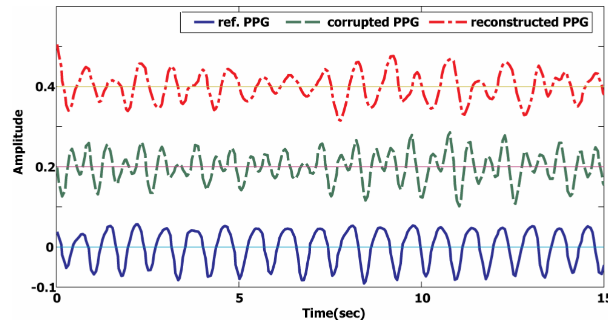

Fig. 7. Reference, corrupted and reconstructed signals

Motion signals of the x and y directions were used in the active noise cancellation algorithm with NLMS (Normal Least Mean Square) algorithm (4th order) to compensate for the corrupted signals. Experiments were conducted on the 1.5 Hz to 2.5 Hz frequency, and the 20 cm moving distance condition during 30 seconds. Fig.7 shows each signal during the experiments.

Data from Fig. 8 shows counted pulses from the Z.C. of each of the signals, and Table I presents error rates among these signals. Error rates, between the measured signal and the reference signal, are higher than 25 %, and at higher frequencies the error rates are also higher. Moreover, when converting these figures to the pulse/min unit, the difference of the Z.C. between the signals is more than 20 pulse/min. However, in the reconstructed signal condition, the error rate is lower than 5% and it can be converted to less than 4 pulse/min.

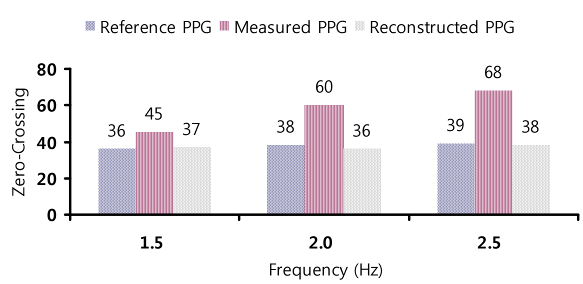

Fig. 8. Pulsation counts from the Z.C. of the signals

TABLE I
ERROR RATES AMONG THE SIGNALS ON VARIOUS FREQUENCIES

	1.5 Hz	2.0 Hz	2.5 Hz
(a)	25.00 %	57.89 %	74.35 %
(b)	2.78 %	5.26 %	2.56 %

(a) Error rate between reference and measured signals
(b) Error rate between reference and reconstructed signals

IV. CONCLUDING REMARKS

Experiments for motion artifact reduction, a major problem of wearable devices, was accomplished with real-time and wireless health monitoring devices. First, we determined the direction of the noise source by comparing signal distortion rates during the three axial directional motions. The x and y axial directional motion was determined as sources of motion artifacts. Next was the motion artifact reduction experiment with signal reconstructed algorithm. The corrupted signal was compensated using two-dimensional active noise cancellation algorithm. Signals were reconstructed from a greater than 25 % error rate to a less than 5% error rate, in conditions with less than 3 Hz motion.

This frequency range is similar to a hand's daily movement. For example, both jogging [9] and hand gestures during conversation [10] have approximately 2 to 3 Hz frequency (see Table Ⅱ). This means that designed wearable devices have the potential to reconstruct the corrupted signal in daily hand motion, and we can obtain accurate pulsation by using the device and stated algorithms.

TABLE II
FREQUENCY OF DAILY HAND MOVEMENT

MOTION	FREQUENCY (HZ)
WALKING	2
RUNNING	3
GESTURE	0 - 4

A : the error rate between reference and measured signals
B : the error rate between reference and reconstructed signals

Looking at daily life, humans are moving more than they are in static conditions such as sleeping. Most accidents and emergencies occur during dynamic movement, so the elderly and other hospital patients are required greater attention during these dynamic conditions. In this case, a wearable health monitoring device, and the motion artifact reduced algorithm techniques, described in this paper, are useful to all individuals, not only patients. The wearable health monitoring device equipped with the motion artifact reduction algorithm can be integrated as a terminal in a so-called ubiquitous healthcare system, which provides a continuous health monitoring without interrupting a daily life.

REFERENCES

[1] J.G.Webster, *Design of Pulse Oximeters*, 1997.

[2] H. H. Asada, P. Shaltis, A. Reisner, S. Rhee, and R. C. Hutchinson, "Mobile monitoring with wearable photoplethysmographic biosensors," *IEEE Eng Med Biol Mag*, vol. 22, pp. 28-40, 2003.

[3] B. S. Kim and S. K. Yoo, "Motion artifact reduction in photoplethysmography using independent component analysis," *IEEE Trans Biomed Eng*, vol. 53, pp. 566-8, 2006.

[4] Y. S. Yan, C. C. Poon, and Y. T. Zhang, "Reduction of motion artifact in pulse oximetry by smoothed pseudo Wigner-Ville distribution," *J Neuroengineering Rehabil*, vol. 2, pp. 3, 2005.

[5] R. V. Philippe Renevey, Jens Krauss, Partrick Celka, Roland Gentsch and Yves Depeursinge, "Wrist-located pulse detection using IR signals, activity and nonlinear artifact cancellation," presented at the 23rd Annual EMBS International Conference, Istanbul, Turkey, 2001.

[6] K. W. Chan and Y. T. Zhang, "Adaptive reduction of motion artifact from photoplethysmographic recordings using a variable step-size LMS filter," 2002.

[7] H. Harry Asada, H. H. Jiang, and P. Gibbs, "Active noise cancellation using MEMS accelerometers for motion-tolerant wearable bio-sensors," *Conf Proc IEEE Eng Med Biol Soc*, vol. 3, pp. 2157-60, 2004.

[8] S. M. a. M. Kuo, Dennis R., *Active Noise Control Systems : algorithms and DSP implementations*. New York, NY., 1996.

[9] E. Kunesch, F. Binkofski, and H. J. Freund, "Invariant temporal characteristics of manipulative hand movements," *Exp Brain Res*, vol. 78, pp. 539-46, 1989.

[10] Y. X. a. F. Quek, "Hand Motion Gesture Frequency Properties and Multimodal Discouse Analysis," *International Journal of Computer Vision*, vol. 69, pp. 353-371, 2006.